IONIZATION RELAXATION BEHIND SHOCK WAVES IN NITROGEN AT SPEEDS OF 17 TO 25 km/sec

M. B. Zheleznyak

Component concentration profiles and heavy-particle and electron temperature profiles have been obtained. Relaxation times for nitrogen atoms and electrons have been determined.

Ionization relaxation behind shock waves in air was considered in [1-4]. It was predicted [2] and then confirmed experimentally [5] that there is a nonmonotonic dependence of relaxation time on shock speed v_S. The nonmonotonic feature increases at $v_S \approx 9.5$ km/sec, when the ionized components begin to make an appreciable contribution to the enthalpy of the equilibrium gas.

1. The state of the gas behind the shock is described by a system of kinetic equations and the equations expressing the laws of conversion of mass flux, momentum, and energy. The relaxation in nitrogen at speeds of $v_S \approx 20$ km/sec takes place practically in an atomic gas because of the complete dissociation of N_2 molecules in the shock. The kinetic equations are written for N, N^+, and N^{+2} as well as for the translational temperature of the heavy particles T_a and the electron temperature T_e.

The following processes are taken into account:

$$N^+ + 2e \leftrightarrows N + e, \quad N^{+2} + 2e \leftrightarrows N^+ + e \tag{1.1}$$

An expression for the recombination constant of the first reaction was obtained in [6], based on a theory accounting for electron diffusion in energy space, and takes the form

$$\alpha_1^{-1} = 2.3 \cdot 10^{31} \left(\frac{T_e}{R} \right)^{9/2} \left[1 + \frac{2\Lambda^* \Sigma_i e^{-E_2/T_e}}{3\sqrt{\pi} g_1 \Lambda} \left(\frac{R}{T_e} \right)^{3/2} \frac{\Delta E_1}{T_e} \right] \tag{1.2}$$

Here R is the Rydberg constant, Λ is the Coulomb logarithm for bound states of the atom (it is calculated using the cross sections for transitions between levels obtained in the Bethe-Born approximation and also takes account of existing experimental data), Σ_i is the state sum of the ion, g_1 is the statistical weight of the atom ground state, E_2 is the energy of the first excited state of the atom, ΔE_1 is the energy difference between the ground state and the first excited state (energy is reckoned from the continuum, and the set of main electronic configuration terms* is taken as a single level), and Λ^* is the value of Λ for $\Delta E \approx 3/2\ T_e$.

The recombination constant α_2 for the second reaction was assumed similarly. The appropriate quantities relating to N^+ were substituted into Eq. (1.2). In calculating the Coulomb logarithm for the bound N^+ states, Coulomb-Born cross sections were used [7]. The equilibrium constants for reactions (1.1) were taken from [8].

As was noted in [3, 9], the N (^4S, ^2P, ^2D) atom terms can have an appreciable relaxation time. Therefore for these levels one must write individual kinetic equations in which, in contrast to [3, 9], only electronic collisions are accounted for (the cross sections are given in [10]). The influence of heavy particles on the kinetics of the terms is insignificant in the conditions considered. At the same time the population of N^+ (^3P, ^1D, ^1S) ion terms was taken to be a Boltzmann distribution in T_e. Since the gradients of T_e

---

*In what follows we shall call these simply terms.

Moscow. Translated from Zhurnal Prikladnoi Mekhaniki i Tekhnicheskoi Fiziki, No. 6, pp. 126-130, November-December, 1970. Original article submitted March 9, 1970.

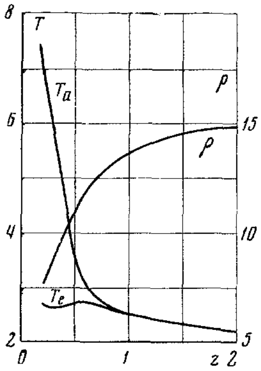

Fig. 1

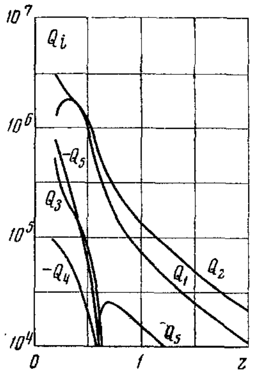

Fig. 2

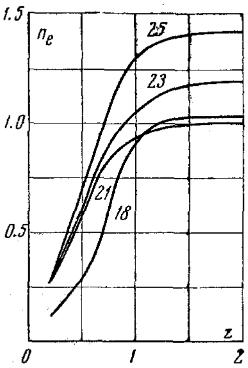

Fig. 3

are small and the electron concentration is significant in the part of the equilibrium zone where N^+ can affect the relaxation appreciably, the concentration of the above terms is close to the Boltzmann value.

The equation for the electron temperature has the form

$$\frac{dT_e}{dx} = \sum_i Q_i \tag{1.3}$$

Here Q_i is the contribution of the i-th process to the electron energy balance. The following processes were taken into account: Q_1 – elastic collisions of electrons with N^+ and N^{+2} ions; Q_2 – the losses in ionization of N atoms and N^+ ions; Q_3 and Q_4 – energy exchange of electrons with terms of N atoms and N^+ ions, respectively,

$$Q_4 = \frac{d(n_{N^+} vE)}{dx}\left(\frac{3}{2} k n_e v\right)^{-1}, \quad Q_5 = \frac{3}{2} T_e \frac{d\ln\rho}{dx} - \frac{T_e}{n_e}\frac{d(n_e v)}{dx} \tag{1.4}$$

Here n_e, n_{N^+} are the concentrations of electrons and N^+ ions, x is the distance from the shock front, v is the gas velocity behind the shock, E is the mean energy of the set of N^+ ion terms, corresponding to a Boltzmann population at the local T_e, and ρ is the density ratio. Expressions for Q_2 and Q_3 are given, for example, in [9], and Q_1 has a standard form.

2. The system of equations given here was integrated numerically on the Minsk-22 computer, using an implicit difference scheme. The profiles of the gas parameters behind the shock were obtained.

Figure 1 shows typical profiles of T_a and T_e, in 10^4°K, and of ρ ($z = xp_1$ in 10^{-4} atm·cm) for a speed $v_s = 21$ km/sec and pressure ahead of the shock of $p_1 = 0.01$ mm Hg.

We now consider the processes determining the T_e profile (Fig. 2, $v_s = 21$ km/sec, $p_1 = 0.01$ mm Hg; the symbols correspond to Eq. (1.3), and Q_i are in 10^4°K/atm·cm). The main processes determining T_e are heating of the electrons due to elastic collisions with ions and losses to ionization by the electron shock. In addition in the initial stage of relaxation, the electrons are heated by energy exchange with terms of N atoms. This arises because the population of the atom terms at first rapidly reaches Boltzmann values near the shock. Later, however, large negative gradients of T_e occur due to loss to ionization, and so the terms cannot adjust to the changing T_e values. This causes heating of the electrons by shocks of the second kind.

Figure 3 shows electron concentration profiles (the numbers indicate v_s in km/sec and n_e in 10^{16} cm^{-3}). In the initial phase of relaxation the reaction to form N^{+2} takes place vigorously. Later the concentration of N decreases, and the contribution of this reaction to the balance of electron generation diminishes. At the same time the rate of formation of N^{+2} increases. The latter process is particularly important for values of v_s for which there is a considerable fraction of N^{+2} in the equilibrium region.

Figure 4 shows the behavior of the N atom concentration. For $v_s \geq 20$ the N concentration passes through a minimum. The reason is that, after the end of the first ionization, the N concentration reaches a state of quasiequilibrium with the system at a temperature exceeding the equilibrium value. As we pass through the second ionization, T_e decreases, and the N^+ recombines, resulting in a decrease of N.

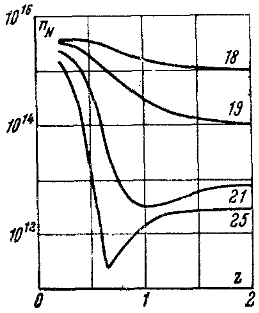

Fig. 4

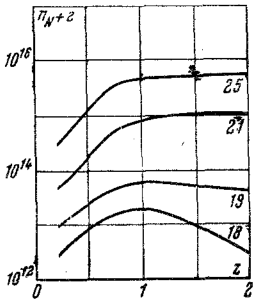

Fig. 5

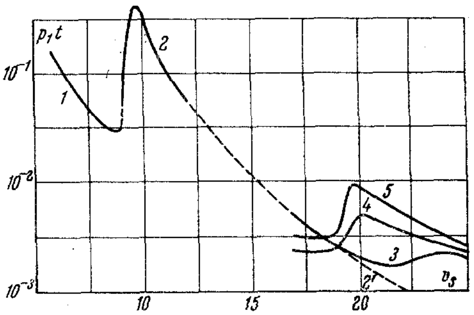

Fig. 6

Figure 5 shows N^{+2} concentration profiles. For speeds $v_s \lessgtr 19.5$ km/sec T_e is of such a value behind the shock that the equilibrium N^{+2} concentrations corresponding to the local values of T_e are small. Therefore, before the end of the first ionization, the N^{+2} value reaches quasiequilibrium with the system for T_e in excess of the equilibrium value. As the first ionization becomes complete, T_e drops, and therefore the N^{+2} concentration decreases. Thus, there is a maximum in N^{+2} for $v_s \lessgtr 19.5$. For $v_s \gtrless 19.5$ km/sec the first ionization proceeds rapidly, and at the final stage of relaxation the system temperature is determined by the second ionization, since the contribution of N^{+2} to the enthalpy of the equilibrium gas becomes insignificant. The result of all this is that the N^{+2} concentration increases monotonically.

We determine the N^{+2} relaxation time similarly to the determination of the ionization time in [1–4], i.e., for $v_s \gtrless 19.5$ km/sec we take the relaxation time to be the time to reach 0.9 of the equilibrium N^{+2} fraction, and for $v_s \lessgtr 19.5$ km/sec we take the time to reach the same fraction of the N^{+2} level at maximum. This determination corresponds to the time for N^{+2} to reach quasiequilibrium with the system, which is complete equilibrium for $v_s \gtrless 19.5$ km/sec. The N^{+2} relaxation time is shown in Fig. 6 as a function of v_s (t in μsec, p_1 in mm Hg; curve 4 is for $p_1 = 0.1$, and curve 5 is for $p_1 = 0.01$), and it can be seen that it depends nonmonotonically on the speed.

Figure 6 also shows the time for ionization relaxation (curve 3), determined as the time to reach 0.9 of the equilibrium degree of ionization. Since the contribution of N^{+2} to the electron balance is small for $v_s < 20$ km/sec, the ionization time is determined by N^+ relaxation. For $v_s > 23$ km/sec the N^{+2} concentration becomes significant, and the ionization time is then determined by N^{+2} relaxation. Since the N^+ relaxation time (curves 2 and 2') and the N^{+2} relaxation time (curves 4 and 5) have a different dependence on v_s, the result is a change in the dependence and in the ionization time in going from low to high speeds. From the concentration and temperature profiles behind the shock one can calculate the radiation from the nonequilibrium region.

By way of example we consider the radiative intensity profiles in the spectral lines of the N^+ ion, which are determined by the concentrations in the excited levels. Behind the shock the gas is not in ionizational equilibrium, and so the population of the excited states will not be the Boltzmann values at local T_e.

In this case, to calculate the populations of the N^+ levels one must use an expression analogous to that obtained in [11] for atoms:

$$n_k = n_k^\circ \left(r_{1k} \frac{n_1}{n_1^\circ} + r_{ke} \frac{n_e n_{N+2}}{n_{N+} K} \right) \qquad (r_{ke} = 1 - r_{1k}) \tag{2.1}$$

Here n_k is the population in the k-th level of N^+; the degree symbols indicate population values corresponding to Boltzmann values at the local T_e; and K is the ionization equilibrium constant for the $N^+ \rightleftharpoons N^{+2} + e$ reaction. The coefficients r_{1k} and r_{ke} determine the relation between the level k and the ground state and the continuum; they are given in explicit form in [11]. The value of r_{1k} depends slightly on temperature and falls off rapidly with increase of k. For k = 2, r_{12} has the largest value ($r_{12} \approx 0.1$).

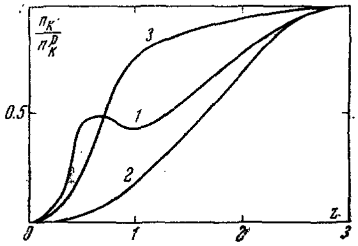

Fig. 7

Figure 7 shows the ratio n_k/n_k^p for $v_s = 21$ km/sec and $p_1 = 0.01$ mm Hg (n_k^p is the population of the k-th level in the equilibrium region) for the 3s levels (k = 2, curve 1) and the highly excited state ($k \gg 1$, curve 2). The maximum in the 3s-level population arises from T_e in the nonequilibrium region exceeding the equilibrium value of T_e. The profiles of n_k/n_k^p for the remaining levels fall between curves 1 and 2. Figure 7 shows the ratio of the nonequilibrium radiative intensity to the equilibrium value in the infrared, for $\lambda \gtrsim 2\,\mu$ (curve 3).

Analogous results were obtained for other values of $v_s > 20$ km/sec.

For $v_s < 20$ km/sec the radiative profiles in the N^+ spectral lines ahead of the N^{+2} maximum are similar to that shown in Fig. 7. After the maximum, because of recombination of N^{+2}, the population of the excited N^+ states can exceed the Boltzmann values for the local T_e, i.e., $n_k > n_k^\circ$. Reduction of T_e upon relaxation leads to a reduction of n_k° and, therefore, to the appearance of a maximum in the n_k populations.

3. We consider the effect of the assumptions made here on the results of the calculations.

No account was taken in the calculations of the contribution of radiative processes to the relaxation kinetics behind the shock. Estimates show that photoionization of ions and atoms does not contribute appreciably to the balance of electron production. Also, precursor effects associated with radiation in advance of the shock can be appreciable.

In this paper we have not considered the state of the gas in the viscous shock layer, whose thickness can be commensurate with that of the nonequilibrium region [12] in the conditions examined. A Maxwellian distribution of heavy-particle velocities becomes established in the viscous shock layer, and there can also be appreciable dissociation of N_2 molecules and ionization [13]. The calculation also ignored heat conduction of the electron gas. It was shown in [14] for higher speeds that this process affects the T_e profile, particularly ahead of the shock. The heat-conduction effect is less for lower shock speeds, and for the conditions of the present paper its role is less, because the state of the gas only behind the shock is considered. Thus, because of photoionization ahead of the shock and ionization in the shock layer, the electron concentration in the shock layer can be appreciable. However, estimates indicate that it will nevertheless be substantially less than the equilibrium degree of ionization.

For the shock waves in air with $v_s < 12$ km/sec examined in [1-4], the chief source of the seed electrons required for the development of ionization by the electron shock wave is associative ionization. For larger speeds its importance decreases because of the existing initial ionization; the avalanche-type process of ionization by the electron shock with large gradients of n_e can begin from the front, the result being that the solution does not depend much on the initial conditions. The profiles of the gas parameters obtained for different initial values of n_e and T_e differ only in a narrow region near the shock front.

It should also be noted that the results depend on the recombination constant α_2. When it changes, the N^{+2} relaxation time changes, but the results remain qualitatively unchanged, i.e., the N^{+2} profiles change from nonmonotonic to monotonic with increase of speed, and there is also a change in the manner in which the ionization time depends on the speed.

4. The individual features of the air components manifest themselves mainly in the molecules and do not appear strongly at large speeds. Therefore, the present data on ionization relaxation in nitrogen can be used to estimate ionization in air. Figure 6 shows the dependence of the ionization time in air (curves 1 [1] and 2 [3]) on v_s. It can be seen that there is a change in the nature of the dependence of the ionization time on v_s at speeds such that single or double atomic ions begin to contribute appreciably to the enthalpy and the electron balance of the equilibrium gas. One can also expect a change in the nature of the behavior of ionization relaxation with time for $v_s \approx 40.55$ km/sec etc., corresponding to triple, quadruple, etc. ionizations (the data on the contribution of ions are taken from [8]).

The author thanks A. Kh. Mnatsakanyan for formulating the problem and discussing the results and G. A. Kobzev and I. T. Yakubov for useful discussions.

LITERATURE CITED

1. S. C. Lin and J. D. Teare, "Rate of ionization behind shock waves in air. II. Theoret. interpretations," Phys. Fluids, 6, No. 3, 355 (1963).

2. L. M. Biberman and I. T. Yakubov, "The state of a gas behind a strong shock wave," Teplofiz. Vys. Temp., 3, No. 3, 340 (1965).
3. M. B. Zheleznyak and A. Kh. Mnatsakanyan, "Ionization relaxation behind strong shock waves in air," Teplofiz. Vys. Temp., 3, No. 3 (1968).
4. S. A. Losev and V. A. Polyanskii, "Nonequilibrium ionization of air behind a shock wave at a speed of 10 km/sec," Izv. Akad. Nauk SSSR, Mekhan. Zhidk.i Gaza, No. 1 (1968).
5. J. Wilson, "Ionization rate of air behind high-speed shock waves," Phys. Fluids, 9, No. 10, 1913 (1966).
6. L. M. Biberman, V. S. Vorob'ev, and I. T. Yakubov, "Contribution to the theory of ionization and recombination in a low-temperature plasma," Zh. Éksper. i Teor. Fiz., 56, No. 6 (1969).
7. M. Seaton, "Theory of excitation and ionization by an electron shock," in: Atomic and Molecular Processes [Russian translation], Mir, Moscow (1964).
8. N. M. Kuznetsov, Thermodynamic Functions and Shock Adiabats for Air at High Temperatures [in Russian], Mashinostroenie, Moscow (1965).
9. M. B. Zheleznyak, A. Kh. Mnatsakanyan, and I. T. Yakubov, "Relaxation and nonequilibrium radiation behind shock waves in air," Izv. Akad. Nauk SSSR, Mekhan. Zhidk. i Gaza, No. 4, 161 (1970).
10. K. Smith, R. J. Henry, and P. G. Burke, "Calculations on the scattering of electrons by atom systems with $2p^q$ configurations," Phys. Rev., 157, No. 1 (1967).
11. L. M. Biberman, V. S. Vorob'ev, and I. T. Yakubov, "A contribution to the theory of a nonequilibrium low-temperature plasma," in: The Magnetohydrodynamic Method of Obtaining Electron Energies [in Russian], Énergiya, Moscow (1968).
12. H. Mott-Smith, "The solution of the Boltzmann equation for a shock wave," Phys. Rev., 82, No. 6, 885 (1951).
13. D. L. Chubb, "Ionizing shock structure in a monatomic gas," Phys. Fluids, 11, No. 11, 2363 (1968).
14. N. N. Magretova, N. T. Pashchenko, and Yu. P. Raizer," Structure of a shock wave in which single ionization of atoms occurs," Zh. Prikl. Mekhan. i Tekhn. Fiz., No. 5, 11 (1970).